

# Phenomenological Lagrangian approach to the electromagnetic deuteron form factors

Yubing Dong,<sup>1,2</sup> Amand Faessler,<sup>3</sup> Thomas Gutsche,<sup>3</sup> and Valery E. Lyubovitskij<sup>3,\*</sup>

<sup>1</sup>*Institute of High Energy Physics, Chinese Academy of Sciences, Beijing 100049, People's Republic of China*

<sup>2</sup>*Theoretical Physics Center for Science Facilities (TPCSF), CAS, People's Republic of China*

<sup>3</sup>*Institut für Theoretische Physik, Universität Tübingen, Auf der Morgenstelle 14, D-72076 Tübingen, Germany*

(Received 24 June 2008; published 17 September 2008)

A phenomenological Lagrangian approach is employed to study the electromagnetic properties of the deuteron. The deuteron is regarded as a weakly bound state of the proton and neutron. We construct a general form for the electromagnetic one- and two-body transition operators formulated in terms of the nucleon fields, which are then used in the calculation of the electromagnetic deuteron form factors. One of the two-body operators is responsible for explaining the quadrupole moment form factor. We show that in our approach the data on the deuteron form factors as well as on the differential cross section of elastic electron-deuteron scattering are well explained.

DOI: [10.1103/PhysRevC.78.035205](https://doi.org/10.1103/PhysRevC.78.035205)

PACS number(s): 13.40.Gp, 14.20.Dh, 36.10.Gv

## I. INTRODUCTION

The study of the electromagnetic properties of the deuteron has a long and rich history (for some recent reviews, see, e.g., Refs. [1–4]). The deuteron, as a spin-1 particle, is usually believed to be a weakly bound system of a proton and a neutron with a binding energy  $\epsilon_D \sim 2.22$  MeV. Because the electromagnetic (e.m.) properties of the deuteron can also shed light on the e.m. form factors of the neutron as well as on nuclear effects on the form factors, the study of the deuteron form factors with a e.m. probe is of great interest.

The matrix element for elastic electron-deuteron ( $eD$ ) scattering in the one-photon approximation is

$$\mathcal{M} = \frac{e^2}{Q^2} \bar{u}_e(k') \gamma_\mu u_e(k) \mathcal{J}_\mu^D(p, p'), \quad (1)$$

where  $k$  and  $k'$  are the four-momenta of initial and final electrons and  $\mathcal{J}_\mu^D(p, p')$  is the deuteron e.m. current

$$\begin{aligned} \mathcal{J}_\mu^D(p, p') &= - \left[ G_1(Q^2) \epsilon'^* \cdot \epsilon - \frac{G_3(Q^2)}{2m_D^2} \epsilon \cdot q \epsilon'^* \cdot q \right] (p + p')_\mu \\ &\quad - G_2(Q^2) (\epsilon_\mu \epsilon'^* \cdot q - \epsilon'_\mu \epsilon \cdot q), \end{aligned} \quad (2)$$

where  $m_D$  is the deuteron mass and  $\epsilon(\epsilon')$  and  $p(p')$  are polarization and four-momentum of the initial (final) deuteron with  $q = p' - p$  being the momentum transfer. The three e.m. form factors  $G_{1,2,3}$  of the deuteron are related to the charge  $G_C$ , quadrupole  $G_Q$ , and magnetic  $G_M$  form factors by

$$\begin{aligned} G_C &= G_1 + \frac{2}{3} \tau G_Q, & G_M &= G_2, \\ G_Q &= G_1 - G_2 + (1 + \tau) G_3, & \tau &= \frac{Q^2}{4m_D^2}. \end{aligned} \quad (3)$$

These form factors are normalized at zero recoil as

$$\begin{aligned} G_C(0) &= 1, & G_Q(0) &= m_D^2 Q_D = 25.83, \\ G_M(0) &= \frac{m_D}{m_N} \mu_D = 1.714, \end{aligned} \quad (4)$$

where  $m_N$  is the nucleon mass and  $Q_D$  and  $\mu_D$  are the quadrupole and magnetic moments of the deuteron. Because the deuteron is a spin-1 particle it has three e.m. form factors in the one-photon-exchange (OPE) approximation, due to current conservation and the  $P$  and  $C$  invariance of the e.m. interaction. The three form factors  $G_{E,M,Q}$  can be determined by measuring the unpolarized, elastic  $eD$  differential cross sections and one of polarization observables, like the deuteron polarization tensor

$$\begin{aligned} T_{20} &= - \frac{1}{S \sqrt{2}} \left\{ \frac{8}{3} \tau G_C G_Q + \frac{8}{9} \tau^2 G_Q^2 \right. \\ &\quad \left. + \frac{\tau}{3} \left[ 1 + 2(1 + \tau) \tan^2 \frac{\theta_e}{2} \right] G_M^2 \right\}, \end{aligned} \quad (5)$$

with  $S = A(Q^2) + B(Q^2) \tan^2(\theta_e/2)$ . The two form factors  $A(Q^2)$  and  $B(Q^2)$  are related to the e.m. form factors of the deuteron as

$$A = G_C^2 + \frac{2}{3} \tau G_M^2 + \frac{8}{9} \tau^2 G_Q^2, \quad B = \frac{4}{3} \tau (1 + \tau) G_M^2. \quad (6a)$$

According to the Rosenbluth separation [5], the elastic scattering of an unpolarized electron from the deuteron results in an  $\mathcal{O}(\alpha^2)$  differential cross section [6]  $d\sigma/d\Omega = (d\sigma/d\Omega)_{\text{Mott}} \mathcal{S}$ , where  $\theta_e$  is the electron scattering angle in the laboratory frame of the collision and  $(d\sigma/d\Omega)_{\text{Mott}}$  is the Mott cross section.

The theoretical study of  $eD$  elastic scattering and deuteron e.m. form factors has been performed in different approaches [7–15]: potential models, phenomenological models including quark, meson, and nucleon degrees of freedom, effective field theories, etc. (for an overview see Refs. [1–4]). In the present work we apply a phenomenological Lagrangian approach to study the e.m. form factors of the deuteron. We consider the deuteron as a weakly bound system of proton and neutron. The coupling of the deuteron to its constituents is determined by the compositeness condition  $Z = 0$  [16,17], which implies

\*On leave of absence from Department of Physics, Tomsk State University, 634050 Tomsk, Russia.

that the renormalization constant of the hadron wave function is set equal to zero. Note that this condition was originally also applied to the study of the deuteron as a bound state of proton and neutron [16]. Then it was extensively used in low-energy hadron phenomenology as the master equation for the treatment of mesons and baryons as bound states of light and heavy constituent quarks (see Refs. [18]). In Refs. [19] this condition was used in the application to hadronic molecule configurations of light and heavy mesons.

To study the e.m. form factors of the deuteron, in a first step we employ the empirical e.m. couplings of the photon to the proton (or neutron) in the one-body operators to set up the well-determined part of the photon-deuteron coupling. As a consequence of the nonlocal description of the deuteron bound state direct contact terms are then included to guarantee local gauge invariance of the e.m. interaction. In the last step we introduce additional, phenomenological two-body operators, which are assumed to represent, e.g., meson-exchange currents and in turn imply a  $D$ -wave component in the deuteron wave function. Parameters of two-body operators are deduced from a fit to the available data.

The article is organized as follows. In Sec. II, we discuss the basic notions of our approach: the coupling of the deuteron to its constituents involving the compositeness condition and the derivation of the e.m. one- and two-body operators contributing to the form factors of the deuteron. In Sec. III we discuss the numerical results for the deuteron e.m. form factors as well as the two form factors  $A(Q^2)$  and  $B(Q^2)$  entering in the differential cross section of the  $eD$  elastic scattering. In Sec. IV we give our conclusions.

## II. APPROACH

### A. Deuteron as a proton-neutron bound state

In this section we discuss the formalism for the study of the deuteron interpreted as a hadronic molecule—a weakly bound state of proton and neutron:  $|D\rangle = |pn\rangle$ . We write the deuteron mass  $m_D$  in the form  $m_D = 2m_N - \epsilon_D$ , where  $m_N = m_p = 0.93827$  GeV is the nucleon mass and  $\epsilon_D \simeq 2.22$  MeV is the binding energy. Based on our approach, the coupling of the deuteron to its two constituents (proton and neutron) is

$$\begin{aligned} \mathcal{L}_D(x) &= g_D D_\mu^\dagger(x) \int dy \Phi_D(y^2) p(x+y/2) C \gamma^\mu n(x-y/2) \\ &\quad + \text{H.c.}, \end{aligned} \quad (7)$$

where  $C = \gamma^0 \gamma^2$  is the charge conjugation matrix and  $x$  is the center-of-mass (c.m.) coordinate. The correlation function  $\Phi_D$  characterizes the finite size of the deuteron as a  $pn$  bound state and depends on the relative Jacobi coordinate  $y$ . A basic requirement for the choice of an explicit form of the correlation function is that its Fourier transform vanishes sufficiently fast in the ultraviolet region of Euclidean space to render the Feynman diagrams ultraviolet finite. We adopt the Gaussian form,  $\tilde{\Phi}_D(p_E^2) \equiv \exp(-p_E^2/\Lambda_D^2)$ , for the Fourier transform of the vertex function, where  $p_E$  is the Euclidean Jacobi momentum. Here,  $\Lambda_D$  is a size parameter that characterizes the distribution of the constituents in the deuteron.

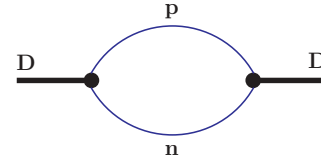


FIG. 1. (Color online) Deuteron mass operator.

The coupling constant  $g_D$  in Eq. (7) is determined by the compositeness condition [16,17], which implies that the renormalization constant of the hadron wave function is set equal to zero:

$$Z_D = 1 - \Sigma'_D(m_D^2) = 0. \quad (8)$$

Here,  $\Sigma'_D(m_D^2) = g_D^2 \Pi'_D(m_D^2)$  is the derivative of the transverse part of the mass operator  $\Sigma_D^{\alpha\beta}$ , conventionally split into the transverse  $\Sigma_D$  and longitudinal  $\Sigma_D^L$  parts as:

$$\Sigma_D^{\alpha\beta}(p) = g_\perp^{\alpha\beta} \Sigma_D(p^2) + \frac{p^\alpha p^\beta}{p^2} \Sigma_D^L(p^2), \quad (9)$$

where  $g_\perp^{\alpha\beta} = g^{\alpha\beta} - p^\alpha p^\beta / p^2$ ,  $g_\perp^{\alpha\beta} p_\alpha = 0$ . The mass operator of the deuteron is described in Fig. 1. For a fixed value of the size parameter  $\Lambda_D$  the coupling  $g_D$  is determined according to the compositeness condition.

To clarify the physical meaning of the compositeness condition, we reiterate that the renormalization constant  $Z_D^{1/2}$  can also be interpreted as the matrix element between the physical and the corresponding bare states. For  $Z_D = 0$  it then follows that the physical state does not contain the bare one and hence the deuteron is described as a bound state of the proton and neutron. As a result of the interaction of the deuteron with its constituents, the deuteron is dressed, i.e., its mass and its wave function have to be renormalized.

Following Eq. (8) the coupling constant  $g_D$  can be expressed in the form:

$$\begin{aligned} \frac{1}{g_D^2} &= \frac{1}{8\pi^2} \int_0^\infty \int_0^\infty \frac{d\alpha d\beta}{(1+\alpha+\beta)^3} \\ &\quad \times \exp \left[ -2(\alpha+\beta)\mu_N^2 + \frac{\alpha+\beta+4\alpha\beta}{2(1+\alpha+\beta)} \mu_D^2 \right] \\ &\quad \times \left\{ (\alpha+\beta+4\alpha\beta) \left[ \mu_N^2 + \frac{1}{2(1+\alpha+\beta)} \right] \right. \\ &\quad \left. + \frac{(1+2\alpha)(1+2\beta)}{4(1+\alpha+\beta)^2} \mu_D^2 \right\} + \frac{(1+2\alpha)(1+2\beta)}{2(1+\alpha+\beta)}, \end{aligned} \quad (10)$$

where  $\mu_H = m_H/\Lambda_D$  with  $H = N, D$ .

### B. Matrix element of the photon-deuteron interaction

To calculate the deuteron e.m. form factors, we construct the electromagnetic transition operator, including one- and two-body parts and formulated in terms of nucleon degrees of freedom—the constituents of the deuteron. Note that the direct coupling of the deuteron with the photon field vanishes

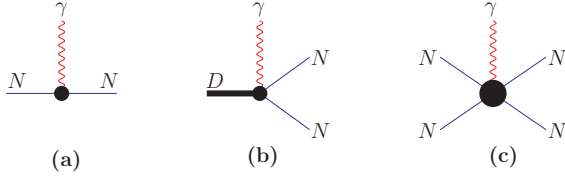


FIG. 2. (Color online) Electromagnetic operators.

because the  $Z_D$  factor equals zero. It guarantees that double counting is avoided.

We construct the one- and two-body operators in a general phenomenological form, which principally includes all possible corrections (e.g., meson-cloud effects) and the dependence on the photon momentum (form factors). The one-body operator (or its Fourier transform) with  $J_\mu^{(1)}(q) = J_\mu^{NN}(q) + J_\mu^{DNN}(q)$  contains two terms. The first term,  $J_\mu^{NN}(q)$ , is generated by the coupling of nucleons to the electromagnetic field:

$$J_\mu^{NN}(q) = \int d^4x e^{-iqx} \bar{N}(x) \left[ \gamma^\mu F_1^N(q^2) + \frac{i\sigma^{\mu\nu} q_\nu}{2m_N} F_2^N(q^2) \right] N(x), \quad (11)$$

where  $F_1^N(q^2)$  and  $F_2^N(q^2)$  with  $N = p, n$  are the conventional Dirac and Pauli form factors of the nucleon [see Fig. 2(a)]. The second term,  $J_\mu^{DNN}(q)$ , is generated by gauging the nonlocal strong Lagrangian  $\mathcal{L}_D$  [see Fig. 2(b)]. To restore electromagnetic gauge invariance in  $\mathcal{L}_D$ , the proton field should be multiplied by the gauge field exponential (see further details in Ref. [18]):

$$p(y) \rightarrow e^{ieI(x,y,P)} p(y), \quad I(x, y, P) = \int_y^x dz_\mu A^\mu(z). \quad (12)$$

For the derivative of  $I(x, y, P)$  we use the path-independent prescription suggested in Ref. [20], which in turn states that the derivative of  $I(x, y, P)$  does not depend on the path  $P$  originally used in the definition. The nonminimal substitution (12) is therefore completely equivalent to the minimal prescription. Expanding the exponential  $e^{ieI(x,y,P)}$  in powers of the electromagnetic field and keeping the linear term (corresponding to the vertex  $D^\dagger p n \gamma + \text{H.c.}$ ) we generate an additional contribution [see Fig. 2(b)] to the electromagnetic one-body operator:

$$J_\mu^{DNN}(q) = -ig_D \int d^4x d^4y D_v^\dagger(x) \Phi_D(y^2) p(x+y/2) \times C \gamma^\nu n(x-y/2) \int_x^{x+y/2} dz_\mu e^{-iqz} + \text{H.c.} \quad (13)$$

There is a number of possible contributions to the two-body operator  $J_\mu^{(2)}(q) = J_\mu^{4N}(q)$ . We restrict to the three simplest terms with the smallest number of derivatives [see the general diagram of Fig. 2(c)]:

$$J_\mu^{4N}(q) = J_\mu^{4N;1}(q) + J_\mu^{4N;2}(q) + J_\mu^{4N;3}(q), \quad (14a)$$

$$J_\mu^{4N;1}(q) = \int d^4x e^{-iqx} g_1 F_1^{NN}(q^2) \bar{n}(x) \gamma^\alpha C \bar{p}(x) \times p(x) C \gamma_\alpha i \sigma_{\mu\nu} q^\nu n(x) + \text{H.c.}, \quad (14b)$$

$$J_\mu^{4N;2}(q) = \int d^4x e^{-iqx} g_2 F_2^{NN}(q^2) \bar{n}(x) \not{q} C \bar{p}(x) \times p(x) C i \sigma_{\mu\nu} q^\nu n(x) + \text{H.c.}, \quad (14c)$$

$$J_\mu^{4N;3}(q) = \int d^4x e^{-iqx} g_3 F_3^{NN}(q^2) [\bar{n}(x) \gamma^\alpha C \bar{p}(x)] \times i(\vec{\partial}_\mu - \overleftarrow{\partial}_\mu)[p(x) C \gamma_\alpha n(x)], \quad (14d)$$

where  $g_i$  and  $F_i^{NN}(q^2)$  are the phenomenological electromagnetic two-body nucleon couplings and form factors, respectively.

To calculate the e.m. form factors of the deuteron we project the dressed operator  $J_\mu(q) = J_\mu^{(1)}(q) + J_\mu^{(2)}(q)$  between the deuteron states:

$$\langle D(p') | J_\mu(q) | D(p) \rangle = (2\pi)^4 \delta^4(p' - p - q) \mathcal{J}_\mu^D(p, p'), \quad (15)$$

where  $\mathcal{J}_\mu^D(p, p')$  is the deuteron e.m. current given by the expression (2). The diagrams contributing to the matrix element (15) are shown in Fig. 3—the diagrams generated by the one-body currents [Figs. 3(a)–3(c)] and by the two-body currents [Fig. 3(d)]. To evaluate these diagrams we take the  $T$  product of the e.m. current in the  $S$  matrix defined in terms of the interaction Lagrangian  $\mathcal{L}_D$  and use the standard free fermion propagators for the nucleons in the loops. Let us stress that a similar approach to the one presented here was previously developed in Ref. [15]. However, in Ref. [15] the authors did not consider two-body operators. Also note that the deuteron e.m. current generated by both the one-body and two-body nucleon operators is manifestly Lorentz covariant and gauge invariant.

We want to point out again that our approach is purely phenomenological in the sense that we do not calculate the one- and two-body operators from microscopic models but constrain their forms using a justified physical background: in particular, the two-body operators (14) introduced in our considerations have an explicit nonrelativistic limit. They correspond to the ones generated in the context of the effective field theory description [14].

The correlation function  $\Phi_D$  of Eq. (7), modeling the distribution of nucleons in the deuteron, has in the full

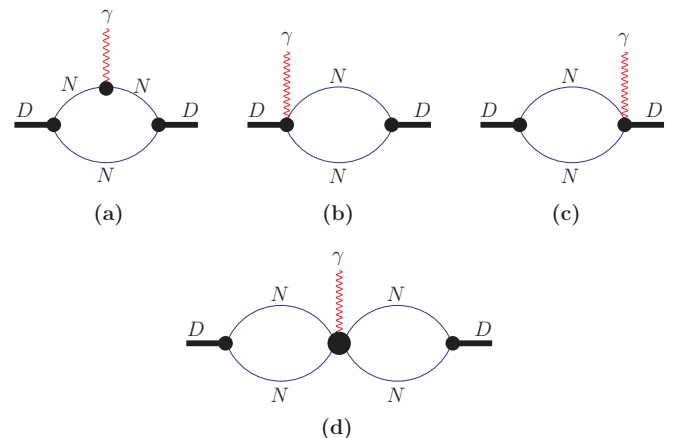


FIG. 3. (Color online) One- and two-body diagrams contributing to the electromagnetic deuteron form factors.

formalism no direct connection to the quantum-mechanical wave function of the deuteron. Comparison of our formalism to the nonrelativistic approaches, dealing with the deuteron wave function, can be performed only on the level of matrix elements. In this vein the expectation value of the two-body operator  $J_\mu^{4N;2}(q)$  between deuteron states incorporates the  $D$ -wave admixture to the deuteron wave function in the context of potential models. This admixture is necessary to explain the quadrupole moment of the deuteron. In the context of effective field theory [14] it was shown before that the nonrelativistic analog of the  $J_\mu^{4N;2}(q)$  operator explains the quadrupole moment/form factor of the deuteron. Therefore, we introduce this operator in consistency with previous observations.

### III. NUMERICAL RESULTS

To describe the e.m. form factors of the deuteron we have the following input: the size parameter  $\Lambda_D$ , describing the distribution of nucleons in the deuteron, the e.m. form factors of the nucleons  $F_{1,2}^{p,n}(q^2)$ , and a set of parameters in the two-body operators—couplings constants  $g_i$  and form factors  $F_i^{NN}(q^2)$ . In fixing the value of the parameter  $\Lambda_D$  we use the following constraint. In the nonrelativistic approximation the vertex function  $\tilde{\Phi}_D(-p^2)$  represents the wave function of the deuteron. Therefore, a constraint condition for  $\Lambda_D$  is set by the deuteron size that, according to potential model calculations, is bound as  $\langle |r^{-2}| \rangle < 0.02 \text{ GeV}^2$  [7]. Employing this condition, we expect that  $\Lambda_D$  is less than 0.5 GeV.

For the set of the e.m. nucleon form factors  $F_{1,2}^{p,n}(q^2)$  we use parametrizations in a fit to the corresponding data. We use two available forms: the Mergell-Meissner-Drechsel (MMD) parametrization [21] and the Kelly parametrization [22]. We stress that when we restrict to the use of one-body transition operators only we cannot reproduce the data on the e.m. form factors of the deuteron. In particular, we cannot correctly predict the  $Q^2$  dependence of the deuteron form factors—the nodes of the charge and magnetic form factors at about 0.7 GeV<sup>2</sup> and 2 GeV<sup>2</sup> [23] are not reproduced. Also, the quadrupole form factor cannot be explained; with the one-body operators present only its normalization is completely underestimated. As is known from potential models [7] the  $D$ -wave component in the deuteron wave function mainly contributes to the quadrupole moment and the quadrupole moment vanishes if only the  $S$ -wave deuteron wave function is considered. Because at this level our correlation function  $\tilde{\Phi}_D(-p^2)$  does not contain an explicit admixture of a  $D$ -wave component, the result for the quadrupole moment with one-body operators is negligibly small when compared to data.

In the present approach we propose and test if a suitable choice for the additional two-body operators can reproduce the full quantitative structure of the deuteron form factors. In particular, as will be shown, the two-body operator  $J_\mu^{4N;2}(q)$  will give the dominant contribution on top of the one-body structures to fully explain the quadrupole form factor. We proceed by fixing the related parameters  $g_2$  and  $F_2^{NN}(q^2)$  of  $J_\mu^{4N;2}(q)$  to reproduce the measured quadrupole form factor of the deuteron. The couplings  $g_{1,3}$  and the form factors  $F_{1,3}^{NN}(Q^2)$  of the additional two-body operators are adjusted to obtain a refined fit to the charge and magnetic form factors, including the nodes at about 0.7 and 2 GeV<sup>2</sup> [23]. For the form factors  $F_{1,2,3}^{NN}(Q^2)$  we use the following parametrization:

$$F_{1,3}^{NN}(Q^2) = \frac{Q^2}{\Lambda^2 + Q^2} \exp\left(-\frac{Q^2}{\Lambda_1^2}\right), \quad (16)$$

$$F_2^{NN}(Q^2) = \frac{\Lambda^2}{\Lambda^2 + Q^2} \exp\left(-\frac{Q^2}{\Lambda_2^2}\right),$$

where  $\Lambda$ ,  $\Lambda_1$ , and  $\Lambda_2$  are the size parameters [for  $F_1^{NN}(Q^2)$  and  $F_3^{NN}(Q^2)$  we use the same ones]. The form factors  $F_1^{NN}(Q^2)$  and  $F_3^{NN}(Q^2)$  should vanish at zero recoil such that the deuteron charge is not renormalized (to preserve the charge conservation), whereas the form factor  $F_2^{NN}(Q^2)$  does not affect current conservation and, therefore, does not vanish at zero recoil. In Table I we present the results for the fit parameters  $g_{1,2,3}$ ,  $\Lambda$ , and  $\Lambda_{1,2}$  using the data on the deuteron e.m. form factors for two different parametrizations [21,22] of the nucleon Dirac and Pauli form factors.

Our numerical results for the deuteron charge, magnetic, and quadrupole form factors as well as for the two form factors,  $A(Q^2)$  and  $B(Q^2)$ , entering in the differential cross section and for the polarization tensor  $T_{20}$  are shown in Figs. 4–18. In particular, in Figs. 4–6 we present the results of our approach for the  $G_C(Q^2)$ ,  $G_Q(Q^2)$ , and  $G_M(Q^2)$  form factors (total contribution of the set of the diagrams in Fig. 3). In Figs. 7–9 we analyze the separate contributions of the graphs of Fig. 3 to  $G_C(Q^2)$ ,  $G_Q(Q^2)$ , and  $G_M(Q^2)$ . In Figs. 10–15 we show the separate contributions of the two-body operators generating the diagram of Fig. 3(d) on a logarithmic scale for  $|G_C(Q^2)|$ ,  $|G_Q(Q^2)|$ , and  $|G_M(Q^2)|$  (Figs. 10, 12, and 14) and on a linear scale for  $G_C(Q^2)$ ,  $G_Q(Q^2)$ , and  $G_M(Q^2)$  (Figs. 11, 13, and 15). In Figs. 16 and 17 we plot our results for the form factors  $A(Q^2)$  and  $B(Q^2)$ . Finally, in Fig. 18 we present the results for the deuteron polarization tensor  $T_{20}(Q^2)$ . We select  $\theta_e = 70^\circ$  to make a comparison consistent with the experimental data. We also perform a comparison with other theoretical calculations. We present our results for the two sets of

TABLE I. Parameters defining the two-body e.m. nucleon operators extracted from data using two forms of the parametrization of the Dirac and Pauli nucleon form factors: MMD [21] and Kelly [22].

$F_{1,2}^{p,n}(Q^2)$	$\Lambda_D$ (GeV)	$g_1$ (fm <sup>4</sup> )	$g_2$ (fm <sup>5</sup> )	$g_3$ (fm <sup>4</sup> )	$\Lambda$ (GeV)	$\Lambda_1$ (GeV)	$\Lambda_2$ (GeV)
MMD [21]	0.25	0.06	-1.97	0.16	1	0.70	0.80
Kelly [22]	0.30	0.23	-1.48	0.06	1	0.58	0.58



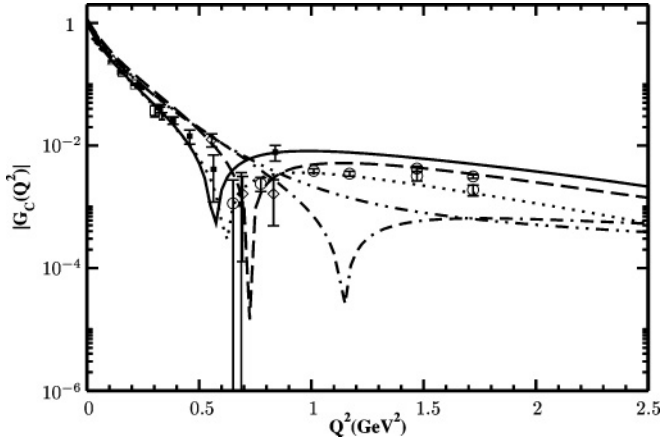


FIG. 4. Form factor  $|G_C(Q^2)|$ . The solid curve is the result of the TGA parametrization. The double dash-dotted and dashed lines are our results with the MMD [21] parametrization restricting to one-body and including two-body electromagnetic currents, respectively. The double dot-dashed and dotted lines are our results with the Kelly [22] parametrization restricting to one-body and including two-body electromagnetic currents, respectively. The data are from Ref. [27] (open circle), Ref. [28] (open square), Ref. [29] (open diamond), Ref. [30] (Plux), Ref. [31] (triangle up), Ref. [32] (filled circle), and Ref. [33] (filled square).

parametrizations of the nucleon e.m. form factors—the MMD [21] and the Kelly parametrization [22]. We also compare our fit to the parametrization derived in Ref. [23] (denoted as TGA parametrization) and data [24–38]. Note that there are several other phenomenological parametrizations for the deuteron e.m. form factors in the literature; see Refs. [24–26]. Our main observations are, first, the one-body diagrams in Figs. 3(a)–3(c) correctly reproduce the normalizations of charge and magnetic form factors. The contribution of the one-body diagrams in Figs. 3(b) and 3(c), generated by gauging the coupling of the deuteron with nucleons, is strongly suppressed in all form factors. They become almost constant at  $Q^2 > 0.5 \text{ GeV}^2$ . Second, the contribution of the one-body diagram of Fig. 3(a) is dominant in the charge and magnetic

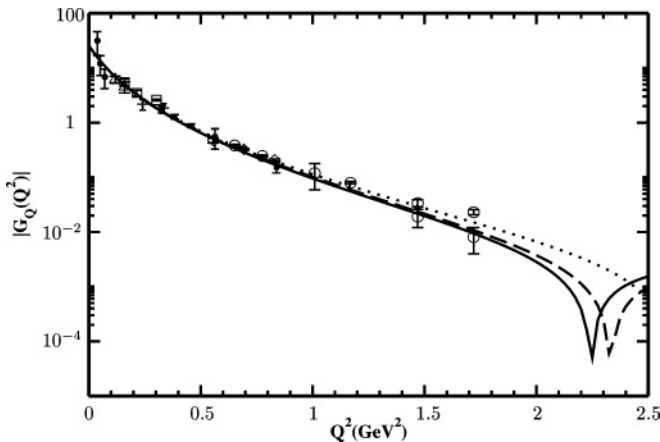


FIG. 5. Form factor  $|G_Q(Q^2)|$ . Notations are the same as described in the caption to Fig. 4.

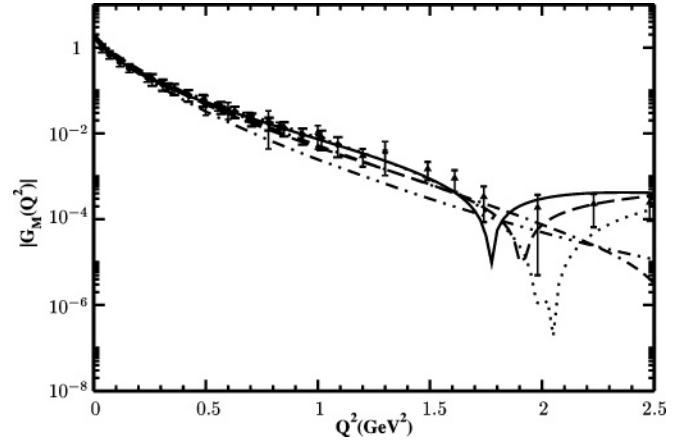


FIG. 6. Form factor  $|G_M(Q^2)|$ . The solid curve is the result of the TGA parametrization. The double dash-dotted and dashed lines are our results with the MMD [21] parametrization restricting to one-body and including two-body electromagnetic currents, respectively. The double dot-dashed and dotted lines are our results with the Kelly [22] parametrization restricting to one-body and including two-body electromagnetic currents, respectively. The data are quoted from Ref. [29] (circle), Ref. [34] (diamond), and Ref. [35] (square), [36] (star).

form factors up to  $1 \text{ GeV}^2$ . Above  $1 \text{ GeV}^2$  the contribution of the two-body operators  $J_{\mu}^{4N;i}$ , generating the diagrams of Fig. 3(d), becomes important for the charge and magnetic form factors. In the case of the quadrupole form factor the contribution of the two-body graph [Fig. 3(d)] generated by the operator  $J_{\mu}^{4N;2}$  is dominant for both the normalization and the  $Q^2$  dependence of this quantity. The operator  $J_{\mu}^{4N;2}$  simulates the contribution of the  $D$ -wave component of the deuteron wave function. Therefore, inclusion of the two-body operators  $J_{\mu}^{4N;i}(q)$  is sufficient to describe the deuteron e.m. form factors as well as elastic  $eD$  scattering. In particular, the two crossing points of the charge and magnetic form factors of the deuteron are also successfully reproduced when including the two-body operators. Without the two-body operators, one cannot

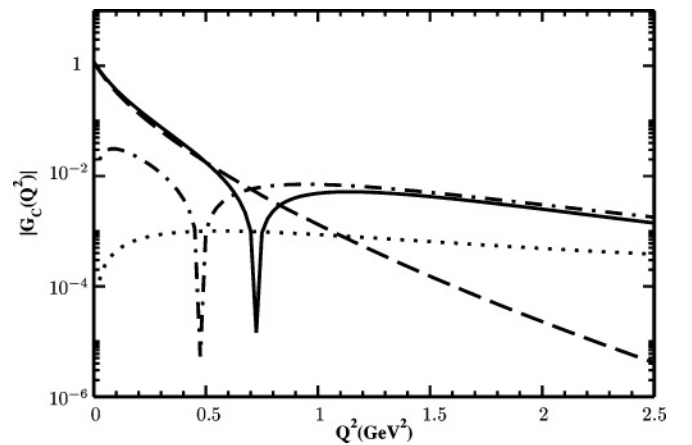


FIG. 7. Form factor  $|G_C(Q^2)|$ . Separate contributions of the diagrams in Fig. 3 with the MMD [21] parametrization: diagram in Fig. 3(a) (the dashed line), diagrams in Figs. 3(b) and 3(c) (the dotted line), the total contribution of two-body operators generating the diagram in Fig. 3(d) (the dot-dashed line).

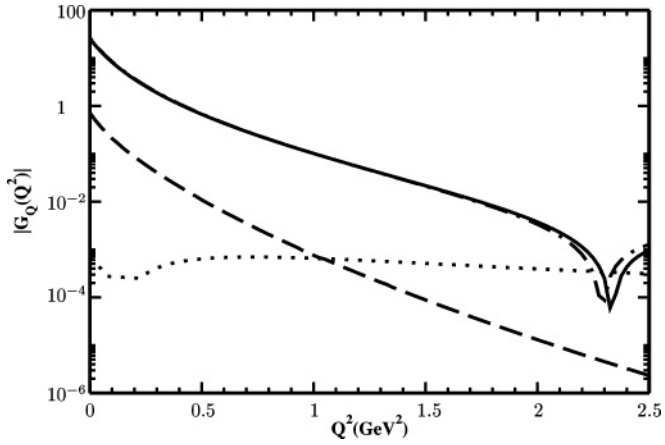


FIG. 8. Form factor  $|G_Q(Q^2)|$ . Separate contributions of the diagrams in Fig. 3 with the MMD [21] parametrization. Notations are the same as described in the caption to Fig. 7.

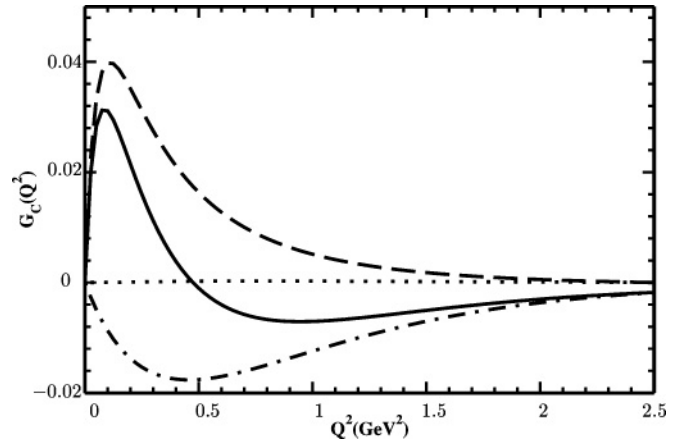


FIG. 11. Form factor  $G_C(Q^2)$  on a linear scale. Separate contributions of the two-body operators with the MMD [21] parametrization. Notations are the same as described in the caption to Fig. 10.

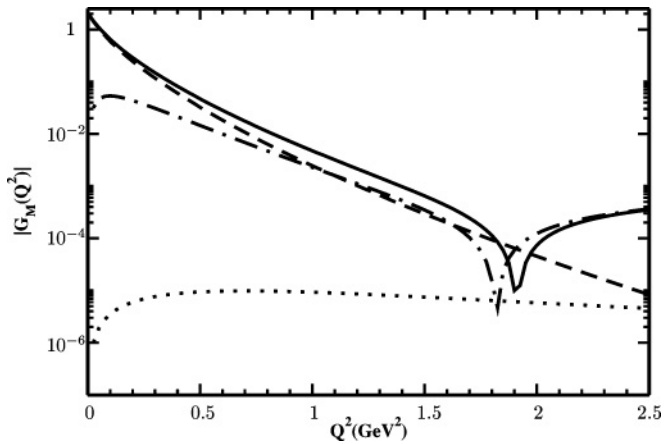


FIG. 9. (Form factor  $|G_M(Q^2)|$ ). Separate contributions of the diagrams in Fig. 3 with the MMD [21] parametrization. Notations are the same as described in the caption to Fig. 7.

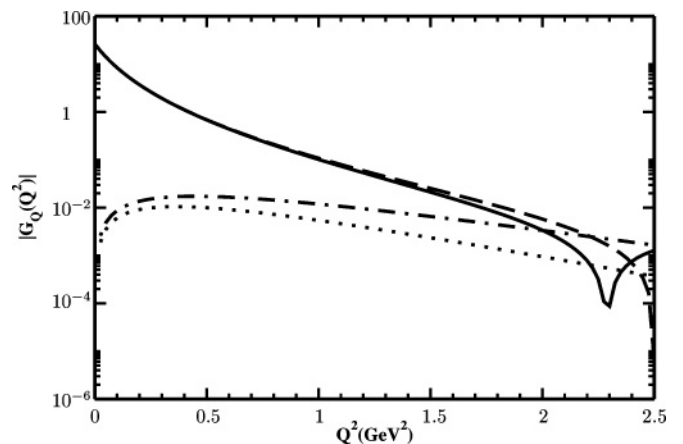


FIG. 12. Form factor  $|G_Q(Q^2)|$ . Separate contributions of the two-body operators with the MMD [21] parametrization. Notations are the same as described in the caption to Fig. 10.

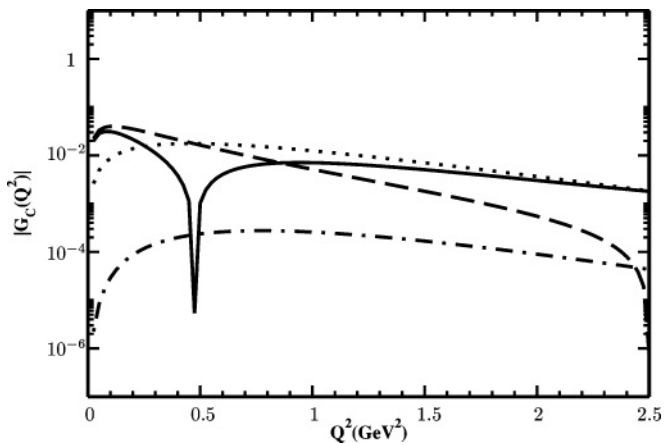


FIG. 10. Form factor  $|G_C(Q^2)|$ . Separate contributions of the two-body operators with the MMD [21] parametrization: the contribution of the  $J_\mu^{4N:1}$  operator (the dotted line), the contribution of the  $J_\mu^{4N:2}$  operator (the dashed line), the contribution of the  $J_\mu^{4N:3}$  operator (the dot-dashed line), and the total result (solid line).

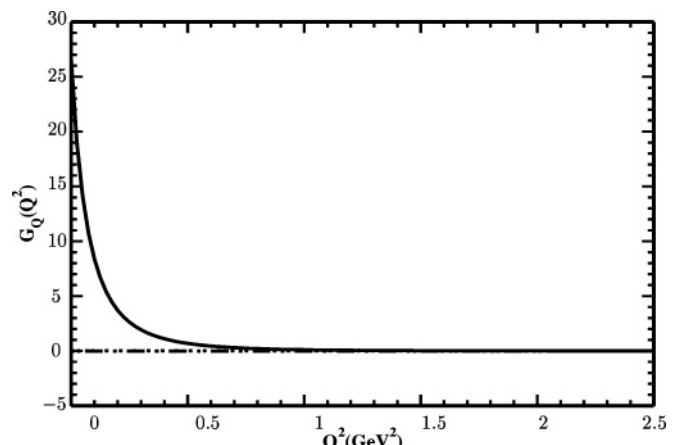


FIG. 13. Form factor  $G_Q(Q^2)$  in a linear scale. Separate contributions of the two-body operators with the MMD [21] parametrization. Notations are the same as described in the caption to Fig. 10.

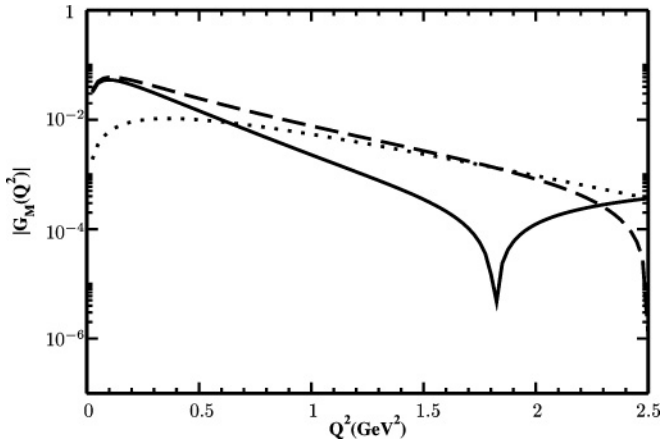


FIG. 14. Form factor  $|G_M(Q^2)|$ . Separate contributions of the two-body operators with the MMD [21] parametrization. Notations are the same as described in the caption to Fig. 10.

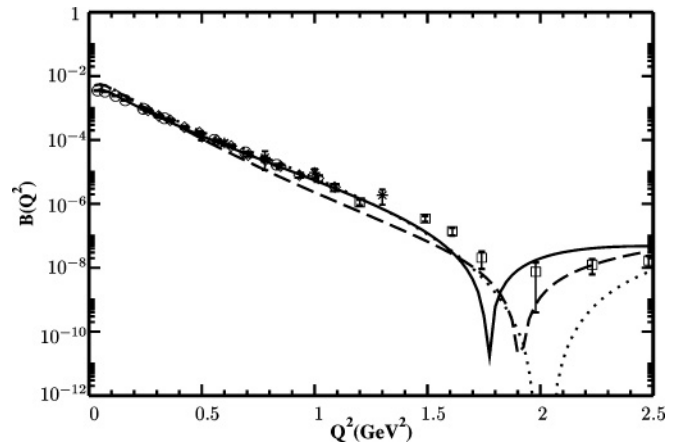


FIG. 17. Form factor  $B(Q^2)$ . Notations are the same as described in the caption to Fig. 16.

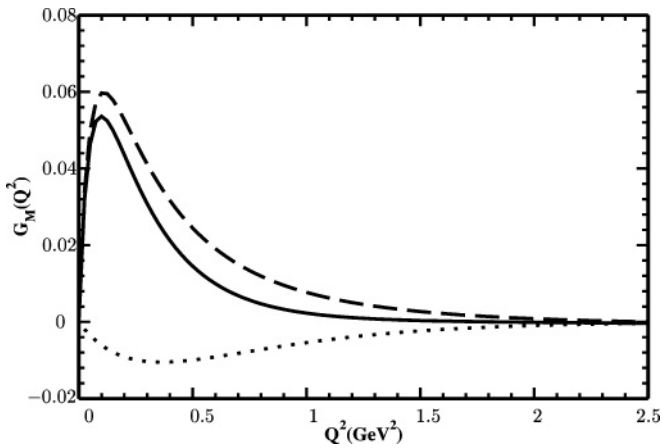


FIG. 15. Form factor  $G_M(Q^2)$  on a linear scale. Separate contributions of the two-body operators with the MMD [21] parametrization. Notations are the same as described in the caption to Fig. 10.

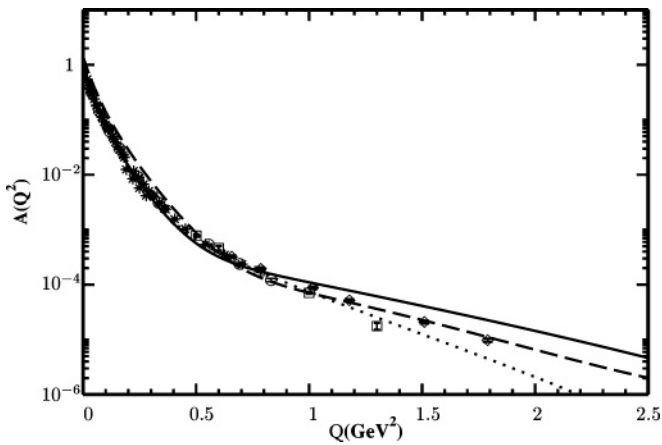


FIG. 16. Form factor  $A(Q^2)$ . The solid curve is the result of the TGA parametrization. The dashed and dotted lines are our results with the MMD [21] and Kelly [22] parametrizations, respectively. The data are quoted from Ref. [29] (circle), Ref. [37] (diamond), Ref. [36] (square), Ref. [38] (star), respectively.

correctly reproduce the two nodes at  $Q^2 \sim 0.7 \text{ GeV}^2$  (for  $G_C$ ) and  $2 \text{ GeV}^2$  (for  $G_M$ ).

We also tested different forms of the deuteron correlation function  $\Phi_D$  (monopole, dipole, Gauss, etc.). It is found that the physical observables are weakly sensitive to its form, whereas they are dominantly controlled by the scale parameter of the correlation function. Inclusion of additional terms (e.g., with derivatives) in the Lagrangian, describing the bound state structure of the deuteron [see Eq. (7)], does not lead to a considerable improvement in the description of the deuteron observables; it only introduces additional parameters. Because we are interested in keeping the number of free parameters to a minimum while still obtaining a good fit to the data we restrict

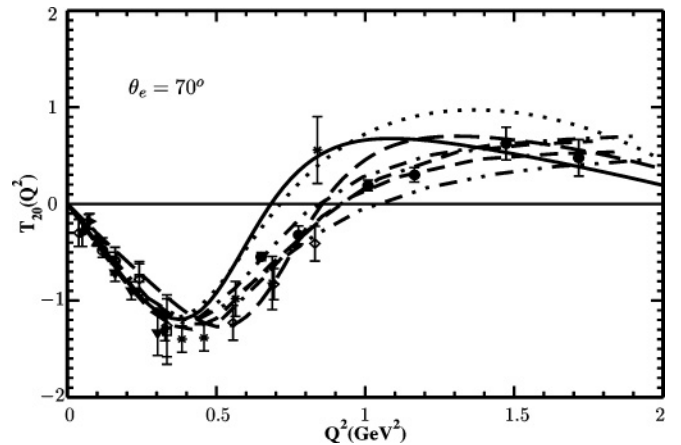


FIG. 18. Deuteron polarization tensor  $T_{20}(Q^2)$  at  $\theta_e = 70^\circ$ . The solid curve is the result of the TGA parametrization. The dashed and dotted lines are our results with the MMD [21] and Kelly [22] parametrizations, respectively. The data are quoted from Ref. [31] (circle), Ref. [39] (triangle right), Ref. [30] (square), Ref. [29] (diamond), Ref. [40] (filled triangle up), Ref. [28] (filled triangle down), Ref. [27] (filled circle), and Ref. [33] (star). The theoretical results are taken from Ref. [8] (dot-dashed line), Ref. [12] (short-dashed line), Ref. [13] (double dash-dotted line), and Ref. [9] (double dotted-dashed line).

the coupling of the deuteron to the constituent nucleons to the simplest form.

#### IV. CONCLUSIONS

In this work, we applied a relativistic effective Lagrangian approach to study the e.m. properties of the deuteron considering the deuteron as a weakly bound state of a proton and a neutron. We found that in the present approach two-body interaction terms are crucial to reproduce the quadrupole moment of the deuteron and the two crossings of the charge and magnetic form factors at  $\sim 0.7$  and  $\sim 2$  GeV<sup>2</sup>, respectively. The effective two-body operators we include reflect and model the  $S/D$  mixing in the deuteron wave function and pion-exchange contributions. With the adjusted parameters, listed in Table I, we obtain a reasonable description of the e.m. form factors of the deuteron up to  $Q^2 \sim 2$  GeV<sup>2</sup> using MMD parametrization of the nucleon e.m. form factors. Note that our result for the deuteron polarization tensor  $T_{20}$  using the MMD parametrization deviates from the data and predictions

of theoretical approaches [8,12,13] in the region  $\simeq 1-1.4$  GeV<sup>2</sup>.

Finally, recent experiments of the electron-proton polarization transfer scattering [41] show that two-photon exchange may play a role for determining the charge form factor of the proton [42]. It is therefore of great interest to check if the two-photon-exchange mechanism also plays a prominent role on the form factors of the deuteron [43] as well as of the neutron. Work along this line is currently in progress.

#### ACKNOWLEDGMENTS

This work was supported by the DFG under Contract Nos. FA67/31-1 and GRK683, National Sciences Foundations Grant No. 10775148, and CAS Grant No. KJXC3-SYW-N2 (Y.B.D.). This research is also part of the EU Integrated Infrastructure Initiative Hadronphysics project under Contract No. RII3-CT-2004-506078 and the President Grant of Russia “Scientific Schools” No. 871.2008.2. Y.B.D. thanks the Tübingen theory group for its hospitality.

- 
- [1] M. Garçon and J. W. Van Orden, *Adv. Nucl. Phys.* **26**, 293 (2001).
- [2] R. Gilman and F. Gross, *J. Phys. G* **28**, R37 (2002).
- [3] I. Sick, *Prog. Part. Nucl. Phys.* **47**, 245 (2001).
- [4] F. Gross, *Eur. Phys. J. A* **17**, 407 (2003).
- [5] M. N. Rosenbluth, *Phys. Rev.* **79**, 615 (1950).
- [6] R. G. Arnold, C. E. Carlson, and F. Gross, *Phys. Rev. C* **21**, 1426 (1980); **23**, 363 (1981).
- [7] J. F. Mathiot, *Phys. Rep.* **173**, 63 (1989); H. Henning, J. J. Adam, P. U. Sauer, and A. Stadler, *Phys. Rev. C* **52**, R471 (1995); J. J. Adam and H. Arenhovel, *Nucl. Phys.* **A614**, 289 (1997).
- [8] R. B. Wiringa, V. G. J. Stoks, and R. Schiavilla, *Phys. Rev. C* **51**, 38 (1995).
- [9] H. Arenhovel, F. Ritz, and T. Wilbois, *Phys. Rev. C* **61**, 034002 (2000).
- [10] M. Gari and H. Hyuga, *Nucl. Phys.* **A278**, 372 (1977); V. V. Burov, S. M. Dorkin, and V. N. Dostovalov, *Z. Phys. A* **315**, 205 (1984); V. V. Burov and V. N. Dostovalov, *Z. Phys. A* **326**, 245 (1987); A. Buchmann, Y. Yamauchi, and A. Faessler, *Nucl. Phys.* **A496**, 621 (1989); H. Ito and L. S. Kisslinger, *Phys. Rev. C* **40**, 887 (1989); E. Hummel and J. A. Tjon, *Phys. Rev. Lett.* **63**, 1788 (1989); G. Ramalho, M. T. Pena, and F. Gross, *Eur. Phys. J. A* **36**, 329 (2008).
- [11] V. A. Karmanov and A. V. Smirnov, *Nucl. Phys.* **A575**, 520 (1994); J. W. Van Orden, N. Devine, and F. Gross, *Phys. Rev. Lett.* **75**, 4369 (1995); J. Carbonell, B. Desplanques, V. A. Karmanov, and J. F. Mathiot, *Phys. Rep.* **300**, 215 (1998); T. W. Allen, W. H. Klink, and W. N. Polyzou, *Phys. Rev. C* **63**, 034002 (2001); T. W. Allen, G. L. Payne, and W. N. Polyzou, *Phys. Rev. C* **62**, 054002 (2000); F. M. Lev, E. Pace, and G. Salme, *Phys. Rev. C* **62**, 064004 (2000).
- [12] J. Carbonell and V. A. Karmanov, *Eur. Phys. J. A* **6**, 9 (1999).
- [13] D. R. Phillips, S. J. Wallace, and N. K. Devine, *Phys. Rev. C* **58**, 2261 (1998).
- [14] D. B. Kaplan, M. J. Savage, and M. B. Wise, *Phys. Rev. C* **59**, 617 (1999); T. S. Park, K. Kubodera, D. P. Min, and M. Rho, *ibid.* **58**, R637 (1998); J. W. Chen, H. W. Griesshammer, M. J. Savage, and R. P. Springer, *Nucl. Phys.* **A644**, 245 (1998); M. Walzl and U. G. Meissner, *Phys. Lett.* **B513**, 37 (2001); D. R. Phillips, *Phys. Lett.* **B567**, 12 (2003); S. R. Beane, M. Malheiro, J. A. McGovern, D. R. Phillips, and U. van Kolck, *Nucl. Phys.* **A747**, 311 (2005); D. Choudhury and D. R. Phillips, *Phys. Rev. C* **71**, 044002 (2005); R. P. Hildebrandt, H. W. Griesshammer, T. R. Hemmert, and D. R. Phillips, *Nucl. Phys.* **A748**, 573 (2005); D. R. Phillips, *J. Phys. G* **34**, 365 (2007); M. P. Valderrama, A. Nogga, E. Ruiz Arriola, and D. R. Phillips, *Eur. Phys. J. A* **36**, 315 (2008).
- [15] A. N. Ivanov, N. I. Troitskaya, M. Faber, and H. Oberhummer, *Phys. Lett.* **B361**, 74 (1995).
- [16] S. Weinberg, *Phys. Rev.* **130**, 776 (1963); A. Salam, *Nuovo Cimento* **25**, 224 (1962); K. Hayashi, M. Hirayama, T. Muta, N. Seto, and T. Shirafuji, *Fortsch. Phys.* **15**, 625 (1967).
- [17] G. V. Efimov and M. A. Ivanov, *The Quark Confinement Model of Hadrons* (IOP Publishing, Bristol/Philadelphia, 1993).
- [18] M. A. Ivanov, M. P. Locher, and V. E. Lyubovitskij, *Few-Body Syst.* **21**, 131 (1996); M. A. Ivanov, V. E. Lyubovitskij, J. G. Körner, and P. Kroll, *Phys. Rev. D* **56**, 348 (1997); M. A. Ivanov, J. G. Körner, and V. E. Lyubovitskij, *Phys. Lett.* **B448**, 143 (1999); M. A. Ivanov, J. G. Körner, V. E. Lyubovitskij, and A. G. Rusetsky, *Phys. Rev. D* **60**, 094002 (1999); A. Faessler, T. Gutsche, M. A. Ivanov, J. G. Körner, and V. E. Lyubovitskij, *Phys. Lett.* **B518**, 55 (2001); A. Faessler, T. Gutsche, M. A. Ivanov, J. G. Körner, V. E. Lyubovitskij, D. Nicmorus, and K. Pumsa-ard, *Phys. Rev. D* **73**, 094013 (2006); A. Faessler, T. Gutsche, B. R. Holstein, V. E. Lyubovitskij, D. Nicmorus, and K. Pumsa-ard, *Phys. Rev. D* **74**, 074010 (2006).
- [19] A. Faessler, T. Gutsche, V. E. Lyubovitskij, and Y. L. Ma, *Phys. Rev. D* **76**, 014005 (2007); A. Faessler, T. Gutsche, S. Kovalenko, and V. E. Lyubovitskij, *ibid.* **76**, 014003 (2007); A. Faessler, T. Gutsche, V. E. Lyubovitskij, and Y. L. Ma, *ibid.* **76**, 114008 (2007); Y. Dong, A. Faessler, T. Gutsche, and V. E. Lyubovitskij, *ibid.* **77**, 094013 (2008).
- [20] S. Mandelstam, *Ann. Phys.* **19**, 1 (1962); J. Terning, *Phys. Rev. D* **44**, 887 (1991).



- [21] P. Mergell, U. G. Meissner, and D. Drechsel, Nucl. Phys. **A596**, 367 (1996).
- [22] J. J. Kelly, Phys. Rev. C **70**, 068202 (2004).
- [23] E. Tomasi-Gustafsson, G. I. Gakh, and C. Adamuscin, Phys. Rev. C **73**, 045204 (2006).
- [24] D. Abbott *et al.* (JLAB t20 Collaboration), Eur. Phys. J. A **7**, 421 (2000).
- [25] A. P. Kobushkin and A. I. Syamtomov, Phys. At. Nucl. **58**, 1477 (1995) [Yad. Fiz. **58**, 1565 (1995)].
- [26] I. Sick and D. Trautmann, Nucl. Phys. **A637**, 559 (1998).
- [27] D. Abbott *et al.* (JLAB t(20) Collaboration), Phys. Rev. Lett. **84**, 5053 (2000).
- [28] M. Bouwuis *et al.*, Phys. Rev. Lett. **82**, 3755 (1999).
- [29] M. Garcon *et al.*, Phys. Rev. C **49**, 2516 (1994).
- [30] R. A. Gilman *et al.*, Phys. Rev. Lett. **65**, 1733 (1990).
- [31] M. E. Schulze *et al.*, Phys. Rev. Lett. **52**, 597 (1984).
- [32] B. B. Voitikhovskiy *et al.*, JETP Lett. **43**, 733 (1986) [Pis'ma Zh. Eksp. Teor. Fiz. **43**, 567 (1986)].
- [33] D. M. Nikolenko *et al.*, Phys. Rev. Lett. **90**, 072501 (2003).
- [34] S. Auffret *et al.*, Phys. Rev. Lett. **54**, 649 (1985).
- [35] P. E. Bosted *et al.*, Phys. Rev. C **42**, 38 (1990).
- [36] R. Cramer *et al.*, Z. Phys. C **29**, 513 (1985).
- [37] D. Abbott *et al.* (Jefferson Lab t(20) Collaboration), Phys. Rev. Lett. **82**, 1379 (1999).
- [38] S. Platchkov *et al.*, Nucl. Phys. **A510**, 740 (1990).
- [39] V. F. Dmitriev *et al.*, Phys. Lett. **B157**, 143 (1985).
- [40] M. Ferro-Luzzi *et al.*, Phys. Rev. Lett. **77**, 2630 (1996).
- [41] M. K. Jones *et al.* (Jefferson Lab. Hall A Collaboration), Phys. Rev. Lett. **84**, 1398 (2000); O. Gayou *et al.* (Jefferson Lab. Hall A Collaboration), *ibid.* **88**, 092301 (2002).
- [42] P. A. M. Guichon and M. Vanderhaeghen, Phys. Rev. Lett. **91**, 142303 (2003); P. G. Blunden, W. Melnitchouk, and J. A. Tjon, *ibid.* **91**, 142304 (2003); Y. C. Chen, A. Afanasev, S. J. Brodsky, C. E. Carlson, and M. Vanderhaeghen, *ibid.* **93**, 122301 (2004); A. V. Afanasev, S. J. Brodsky, C. E. Carlson, Y. C. Chen, and M. Vanderhaeghen, Phys. Rev. D **72**, 013008 (2005); J. Arrington, Phys. Rev. C **68**, 034325 (2003); J. Arrington, Phys. Rev. C **69**, 022201(R) (2004).
- [43] Y. B. Dong, C. W. Kao, S. N. Yang, and Y. C. Chen, Phys. Rev. C **74**, 064006 (2006).